ROYAL SOCIETY OPEN SCIENCE

royalsocietypublishing.org/journal/rsos

Research

Cite this article: Zhang T-t, Yan L-m. 2019 Enhanced low-temperature NH_3-SCR performance of Ce/TiO_2 modified by Ho catalyst. *R. Soc. open sci.* **6**: 182120.
http://dx.doi.org/10.1098/rsos.182120

Received: 18 December 2018
Accepted: 6 February 2019

Subject Category:
Chemistry

Subject Areas:
environmental chemistry/chemical physics

Keywords:
Ce/TiO_2, Ho doping, SO_2 resistance, low-temperature NH_3-SCR

Author for correspondence:
Li-min Yan
e-mail: yanlm@shu.edu.cn

This article has been edited by the Royal Society of Chemistry, including the commissioning, peer review process and editorial aspects up to the point of acceptance.

Electronic supplementary material is available online at https://dx.doi.org/10.6084/m9.figshare.c.4418234.

THE ROYAL SOCIETY PUBLISHING

Enhanced low-temperature NH_3-SCR performance of Ce/TiO_2 modified by Ho catalyst

Ting-ting Zhang and Li-min Yan

Shanghai University Microelectronic R&D Center, Shanghai University, Shanghai 200072, People's Republic of China

L-mY, 0000-0001-6777-0075

Holmium was used as a dopant to boost the low-temperature NH_3-selective catalytic reduction (SCR) performance of Ce/TiO_2 catalyst. It was ascertained that certain amount of Ho-doping species could exceedingly improve the low-temperature SCR activity under 60 000 h^{-1} of Ce/TiO_2, accompanied with the improvement of tolerance to H_2O and SO_2 at 200°C. Characterization results manifested that Ho modification could not only result in inhibiting the growth of TiO_2 crystals and the enlargement of specific surface area but also lead to the enhanced redox ability and the increased amount of surface-adsorbed substances, all of which could promote the low-temperature NH_3-SCR performance of Ce/TiO_2.

1. Introduction

Lately, NOx has become one of the significant sources of air pollution. The over-standard concentration of NOx emission was mainly caused by the combustion process of fossil fuel, which has caused many environmental problems such as city smog and pollution [1–4]. Selective catalytic reduction (SCR) is the widely accepted de-NOx technology, and V_2O_5-WO_3 (MoO_3)/TiO_2 catalyst is the most commercially used catalyst in this SCR system [5]. However, there are still some disadvantages in the SCR system with V_2O_5-WO_3 (MoO_3)/TiO_2, such as the high operating temperature (300–400°C), the toxicity of vanadium species, low N_2 selectivity in the working temperature range [6–9]. Based on these practical disadvantages, it is necessary to study non-vanadium catalysts with better low-temperature SCR performance.

Cerium, one of the most abundant rare-earth metals, has drawn attention due to the high oxygen storage capacity and good redox property. It has been widely applied in catalysis, such as carbon monoxide oxidation and reforming reactions [10–12]. Results of previous research proved that cerium-based oxide catalysts had a good SCR performance. Gao *et al*. [13] reported that Ce/TiO_2 by the sol–gel method possesses high

© 2019 The Authors. Published by the Royal Society under the terms of the Creative Commons Attribution License http://creativecommons.org/licenses/by/4.0/, which permits unrestricted use, provided the original author and source are credited.

surface area and good redox ability, contributing to its high SCR activity. Vuong *et al*. [14] reported that $V/CeTiO_2$ catalysts showed excellent de-NOx activity at low temperature. Notably, the best one of these $V/CeTiO_2$ catalysts showed almost 100% NO conversion at 190°C. It was also found [15] that doping certain quantity of Ca would increase Ce^{3+} and surface-adsorbed oxygen. Meanwhile, the Brønsted acidity and redox ability were also greatly enhanced. All these factors may be responsible for the enhanced activity. Mosrati [16] recently reported that an impregnated Ce/Ti oxide catalyst with Nb modification presents a 95% NOx conversion at 200°C. Relevant characterization results proved that the Nb introduction decreases the surface area and strengthens the surface acidity. A Ce–Ti oxide catalyst with Cu addition could promote the SO_2 resistance of Ce–Ti oxide [17]. Although several catalysts, such as $V/CeTiO_2$ and $Ce–Cu–TiO_2$, have been successfully applied in NH_3-SCR, enhanced low-temperature NH_3-SCR performance and SO_2 resistance of Ce/TiO_2 modified by Ho have never been reported.

As a rare earth metal, Ho has been successfully applied for improving the photocatalytic activity of TiO_2 [18]. Owing to its electron trap effect of $Ho^{2+} \leftrightarrow Ho^{3+}$, the doping of Ho could efficiently enhance the photocatalytic ability of TiO_2. Gamal *et al*. [19] reported that the surface of Ho_2O_3 exposes more Lewis acid sites, which play a vital role in NH_3-SCR reaction. It was also reported [20] that Ho-modified $Fe–Mn/TiO_2$ catalyst shows a larger specific area of Fe_2O_3 phase compared with that of $Fe–Mn/TiO_2$, which results in a board temperature window and high SO_2 tolerance in NH_3-SCR reaction. However, the investigation of Ce/TiO_2 catalyst with Ho addition has not been reported. In this work, Ho is used for improving the low-temperature NH_3-SCR activity of Ce/TiO_2, and several characterization methods were applied for investigating the promotion mechanism. Furthermore, $SO_2 + H_2O$ tolerance of the best catalyst was also studied.

2. Experimental

2.1. Catalyst preparation

The impregnation method was used to prepare the catalysts. Titanium dioxide (anatase, 0.05 mol) was impregnated with cerium nitrate (0.0175 mol) and holmium nitrate in 100 ml deionized water, followed by stirring at 20°C for 3 h. The obtained mixture was dried for 12 h at 100°C and then calcined at 500°C for 4 h. The prepared samples were labelled as $Ce_{0.35}/TiO_2$ and $Ho_xCe_{0.35}/TiO_2$ (the molar ratios of Ho/Ti and Ce/Ti were x and 0.35, respectively).

2.2. Catalyst characterization

Powder X-ray diffraction (XRD) patterns were obtained on a Philips X'pert Pro diffractometer with Ni-filtered Cu Kα radiation (0.15408 nm). 2θ ranged from 10° to 80° with a step size of 0.02°.

The specific surface area was measured by N_2 adsorption at −196°C, using an ASAP 2020 volumetric adsorption analyser. Before each precise test, the catalysts were evacuated for 3 h at 300°C. The specific surface area and the pore volume of the samples were calculated by the Brunauer–Emmett–Teller (BET) method and the pore size distributions were derived from the adsorption branches of the isotherms using the Barrett–Joyner–Halenda model.

The H_2 temperature-programmed reduction (TPR) experiments were performed on a Micromeritics AutoChem 2920 chemisorption analyser. Typically, 0.1 g sample was pretreated in pure N_2 at 400°C for 0.5 h and then cooled to 20°C followed by N_2 purging for 0.5 h. The temperature was heated by 10°C min^{-1} from 100 to 800°C in 10 vol% H_2/Ar. Thermal conductivity detector monitored H_2 consumption in this progress.

The NH_3 temperature-programmed desorption (TPD) experiments were carried out on the same equipment as the TPR experiment. As a pretreatment step, 0.1 g samples were purged at 400°C in N_2 for 0.5 h and cooled to 30°C. Then the samples were purged in NH_3 for 1.0 h. At last, the programmed desorption was carried out at the rate of 10°C min^{-1} (100–500°C) in Ar.

In situ diffuse reflectance infrared Fourier transform spectroscopy (DRIFTS) experiments were carried out on a Nicolet 6700 FTIR spectrometer with an MCT/A detector. As a pretreatment step, the catalysts were treated at 450°C in N_2 for 0.5 h and cooled to 50°C. Background spectra were recorded in the N_2 flow and automatically subtracted from the corresponding spectra. The spectra were recorded by accumulating 64 scans at a 4 cm^{-1} resolution.

2.3. Catalytic activity test

SCR activity experiments were performed in a fixed-bed reactor containing 0.4 g catalysts (40–60 mesh) with a GHSV of 60 000 h^{-1}. The total gas flow was 200 ml min^{-1}, which was premixed in a gas mixer to obtain the simulated gas of [NO] = [NH_3] = 500 ppm, [O_2] = 3 vol.%, [H_2O] = 8 vol.% (when used), [SO_2] = 200 ppm (when used) and balanced by N_2. Then the mixed gas went into the reactor and the NO and NO_2 concentrations were monitored by a 350-XL flue gas analyser. The experiment data were recorded from 100 to 400°C at a steady state. The formulae for NO_x conversion and N_2 selectivity were as follows:

$$NO_x \text{ conversion } (\%) = \frac{[NO_x]_{in} - [NO_x]_{out}}{[NO_x]_{in}} \times 100\% \tag{2.1}$$

$$N_2 \text{ selectivity} = \left(1 - \frac{2[N_2O]_{out}}{[NOx]_{in} + [NH_3]_{in} - [NOx]_{out} - [NH_3]_{out}}\right) \times 100\%. \tag{2.2}$$

Also, NO oxidation conversion was also tested in the same fixed-bed reactor in the same simulated flue gas components without NH_3.

3. Results and discussion

3.1. Catalytic performance

The NOx conversions of various catalysts are plotted as a function of temperature, as exhibited in figure 1*a*. Among the prepared catalysts, $Ce_{0.35}/TiO_2$ and $Ho_{0.35}/TiO_2$ showed a limited de-NOx activity (less than 80%) in the entire temperature scope. It is notable that the low-temperature (less than 200°C) catalytic activity of $Ce_{0.35}/TiO_2$ was much improved when small amounts of Ho species are doped, as evidenced by the NO conversion of $Ho_{0.15}Ce_{0.35}/TiO_2$. When the Ho/Ti molar ratio rises to 0.45, the NOx conversion over $Ce_{0.35}/TiO_2$ at 150°C was also increased from 22% to 56%. However, further increasing of Ho/Ti molar ratio to 0.6 led to a slight decrease of de-NOx activity in the whole temperature range. Figure 1*b* shows the N_2 selectivity as a function of temperature over $Ho_xCe_{0.35}/TiO_2$ catalysts. It could be readily observed that the addition of Ho could enhance the N_2 selectivity of $Ce_{0.35}/TiO_2$ catalyst. Although all prepared catalysts showed high N_2 selectivity in the temperature range of 100–300°C, $Ce_{0.35}/TiO_2$ added with Ho exhibited relatively better N_2 selectivity above 300°C compared with $Ce_{0.35}/TiO_2$ catalyst.

3.2. Tolerance of SO_2 and H_2O

In practical applications, trace amounts of sulfur dioxide and water are still contained in the exhaust gas through the desulfurization unit, which may result in the deactivation of the catalyst. Therefore, the effect of SO_2 and water on the SCR activity of the catalyst was studied. Figure 2 depicts the catalytic performance of $Ce_{0.35}/TiO_2$ and $Ho_{0.45}Ce_{0.35}/TiO_2$, as a function of time in the presence of 200 ppm SO_2 and 8 vol.% water at 200°C. As exhibited in figure 2, the NO conversion over $Ce_{0.35}/TiO_2$ decreased from 52% to 33% after introducing $SO_2 + H_2O$ for 200 min, then gradually recovered (37%) after the cut off of $SO_2 + H_2O$ and kept stable during the following test period. By contrast, the presence of $SO_2 + H_2O$ in the feed gas induced a dramatic decrease of NO conversion over $Ho_xCe_{0.35}/TiO_2$ by 10%. After eliminating $SO_2 + H_2O$ from the feed gas, the conversion of NO over $Ho_xCe_{0.35}/TiO_2$ was gradually restored to a certain extent but is less than the initial value (about 72%). All these analyses implied that a better resistance of $SO_2 + H_2O$ could be achieved by Ho modification.

3.3. Brunauer–Emmett–Teller results

BET surface area, total pore volume and average pore were tested. As listed in table 1, the specific surface areas of $Ce_{0.35}/TiO_2$, $Ho_{0.35}/TiO_2$, $Ho_{0.15}Ce_{0.35}/TiO_2$, $Ho_{0.3}Ce_{0.35}/TiO_2$, $Ho_{0.45}Ce_{0.35}/TiO_2$, and $Ho_{0.6}Ce_{0.35}/TiO_2$ are 189.61, 157.34, 196.33, 198.34, 204.56 and 203.65 $m^2\,g^{-1}$, respectively. It is obvious that the specific surface area of $Ho_xCe_{0.35}/TiO_2$ became larger as the Ho/Ti molar ratio increased from 0.15 to 0.45. However, doping excess Ho species to Ce/TiO_2 (Ho/Ti molar ratio = 0.6) may result in a decrease in BET surface area. Considering the SCR activity results from figure 1*a*, Ce/

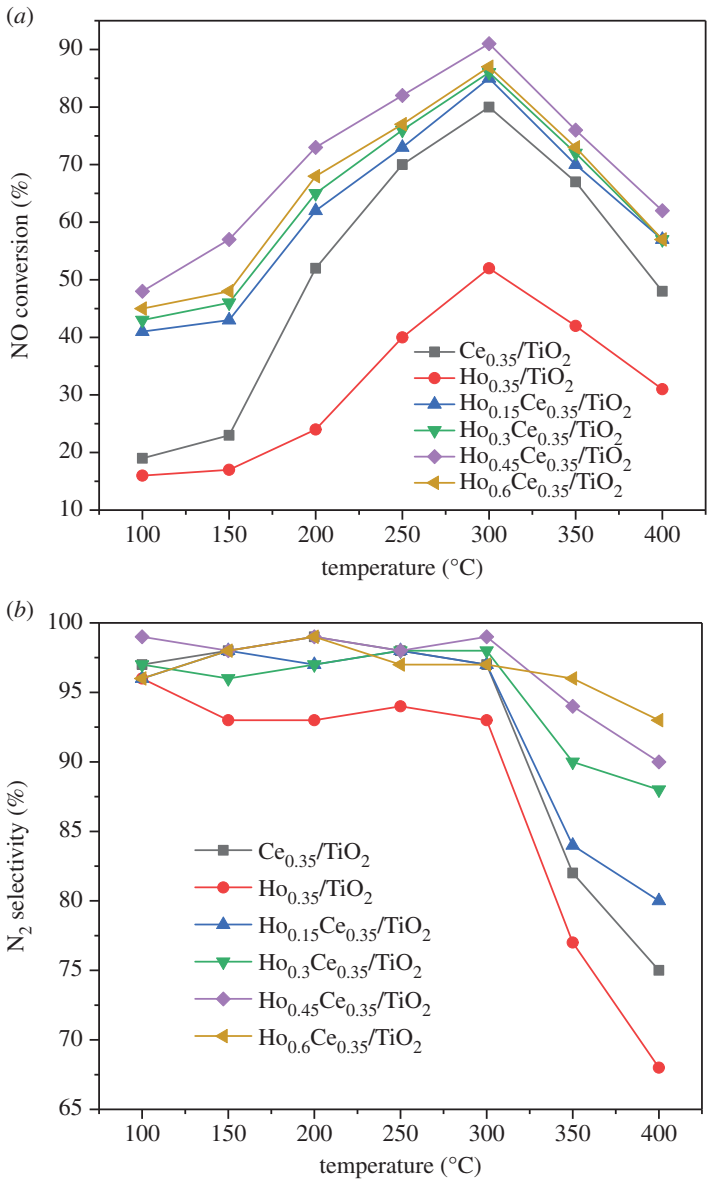

Figure 1. (*a*) NOx conversion and (*b*) N_2 selectivity in the NH_3-SCR reaction over $Ho_xCe_{0.35}/TiO_2$ catalysts (500 ppm NO, 500 ppm NH_3, 3 vol.% O_2, total flow rate 200 ml min^{-1} and GHSV = 60 000 h^{-1}).

TiO_2 with proper Ho species modification may possess higher active surface area, which is beneficial for the effective contacts with reactants.

3.4. Powder X-ray diffraction results

XRD patterns of $Ce_{0.35}/TiO_2$ and $Ho_xCe_{0.35}/TiO_2$ are shown in figure 3. Only diffraction peaks assigned to TiO_2 are detected. Specifically, much anatase-phase TiO_2 (PDF-ICDD21-1272) and a little rutile-phase TiO_2 (PDF-ICDD21-1276) are observed. A similar phenomenon was also reported by Liu *et al.* [21]. It means that Ce and Ho species are highly dispreading on the surface of TiO_2. With the increase of Ho-doping amount, the intensities of all diffraction peaks became weak, suggesting that the introduction of Ho could further reduce the crystallization of TiO_2. All of the factors above are favourable to a good SCR performance.

3.5. X-ray photoelectron spectroscopy results

Figure 4 exhibits the X-ray photoelectron spectroscopy (XPS) spectra of Ce 3d and O 1s over $Ce_{0.35}/TiO_2$ and $Ho_{0.45}Ce_{0.35}/TiO_2$ catalysts. In addition, the XPS spectrum of Ho 4d over $Ho_{0.45}Ce_{0.35}/TiO_2$ has been given in figure 4*c*. Table 2 lists the surface element compositions and their chemical states by the XPS technique.

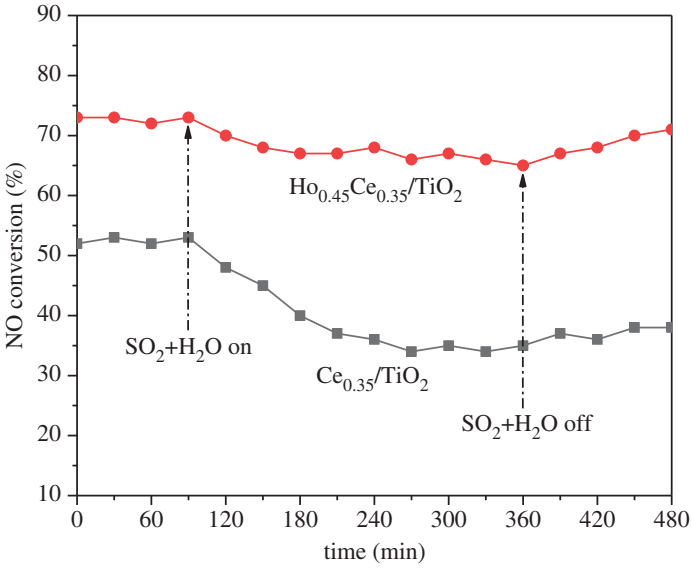

Figure 2. NOx conversion of $Ce_{0.35}/TiO_2$ and $Ho_{0.45}Ce_{0.35}/TiO_2$ in the presence of SO_2 and H_2O at 200°C (500 ppm NO, 500 ppm NH_3, 3 vol.% O_2, 8 vol.% H_2O, 200 ppm SO_2, total flow rate 200 ml min^{-1} and GHSV = 60 000 h^{-1}).

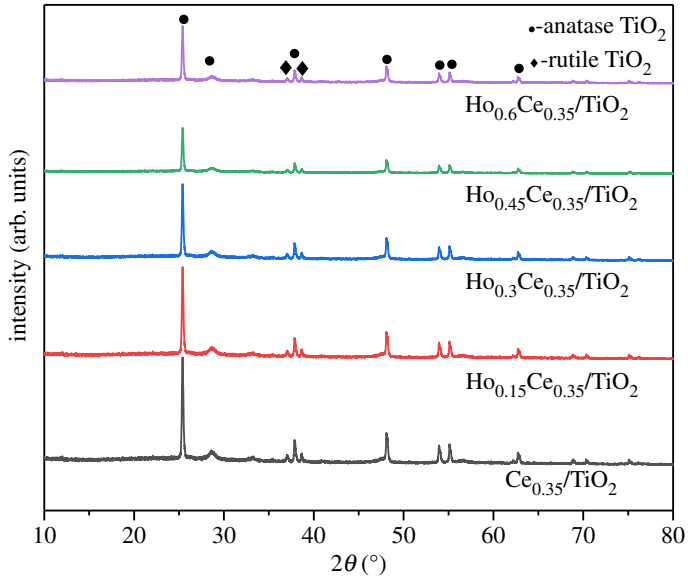

Figure 3. XRD patterns of $Ho_xCe_{0.35}/TiO_2$ catalysts.

Table 1. Textural parameters of the catalysts.

samples	BET surface area (m^2g^{-1})	pore volume ($cm^3\ g^{-1}$)	average pore diameter (nm)
$Ce_{0.35}/TiO_2$	189.61	0.612	9.55
$Ho_{0.35}/TiO_2$	157.34	0.424	7.89
$Ho_{0.15}Ce_{0.35}/TiO_2$	196.33	0.608	9.43
$Ho_{0.3}Ce_{0.35}/TiO_2$	198.34	0.627	9.57
$Ho_{0.45}Ce_{0.35}/TiO_2$	204.56	0.628	9.61
$Ho_{0.6}Ce_{0.35}/TiO_2$	203.65	0.611	9.47

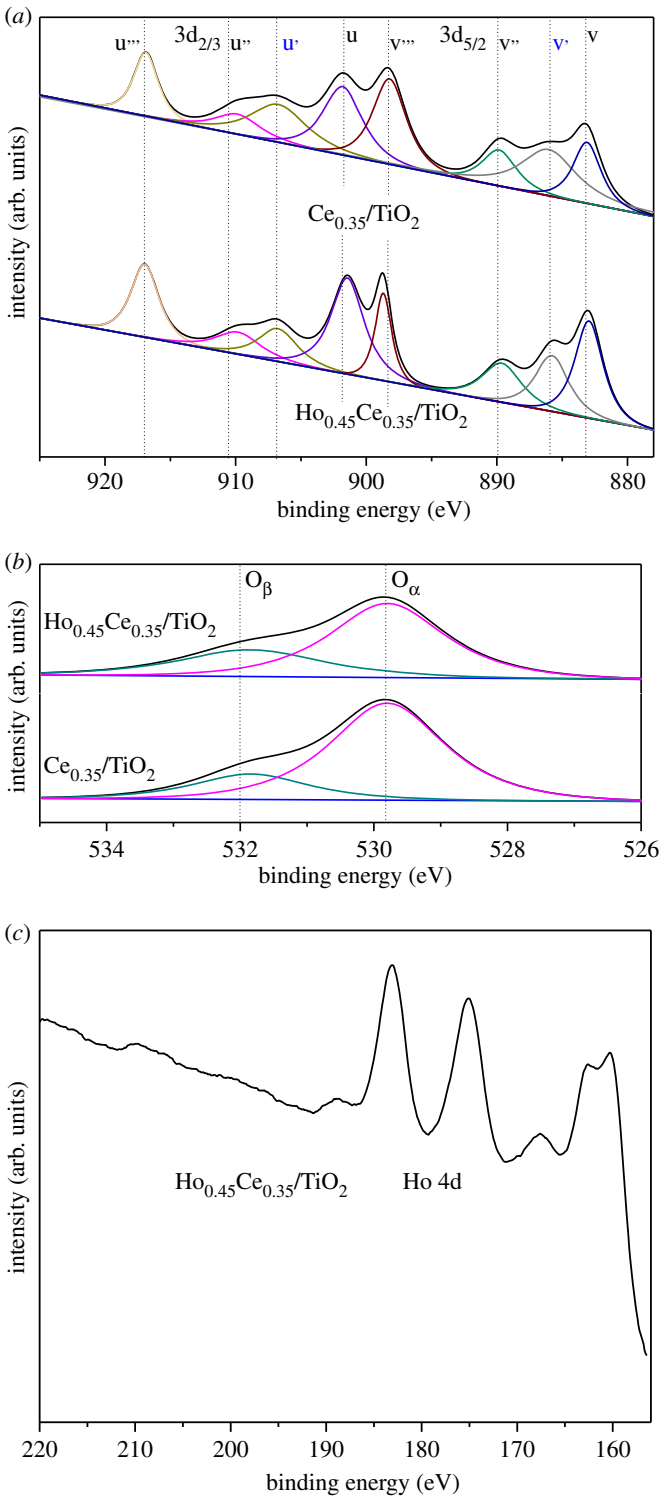

Figure 4. XPS spectra of $Ce_{0.35}/TiO_2$ and $Ho_xCe_{0.35}/TiO_2$ catalysts.

As seen in figure 4*a*, the complicated Ce 3d XPS curves of different samples were made up of eight peaks. u and v peaks belonged to $3d_{3/2}$ and $3d_{5/2}$ spin–orbit components, respectively. u′ and v′ peaks could be attributed to Ce^{3+} and the other peaks could be assigned to Ce^{4+} [22]. These Ce^{3+} /Ce^{4+} pairs over the catalyst surface were beneficial for not only the storage and release of active oxygen species but also the oxidation of NO to NO_2 [23]. Additionally, more Ce^{3+} would promote the generation of more oxygen vacancies, which help to adsorb reactants [24,25]. The factors mentioned above proved to contribute to the progress of the SCR reaction. Thus, it is necessary to study the ratio of $Ce^{3+}/(Ce^{3+} + Ce^{4+})$ over the selected catalysts. The ratio of $Ce^{3+}/(Ce^{3+} + Ce^{4+})$ was calculated according to the

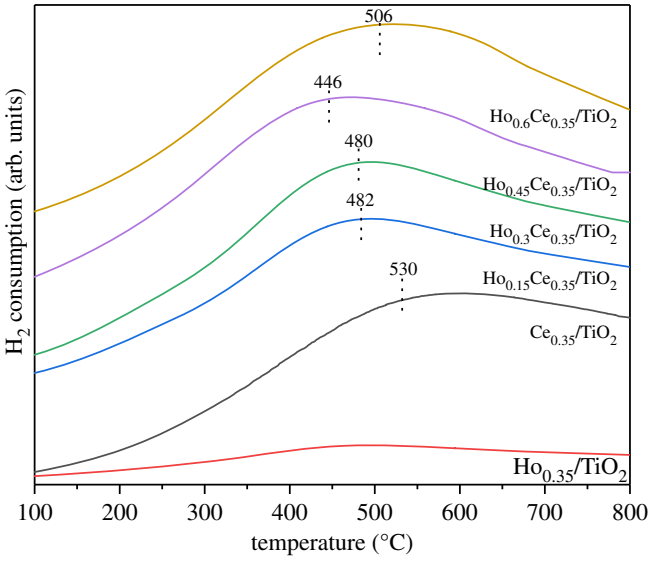

Figure 5. H_2-TPR patterns of $Ho_xCe_{0.35}/TiO_2$ catalysts.

Table 2. Surface elemental analysis by XPS.

	atomic concentration (%)					
samples	Ce	Ti	O	Ho	$Ce^{3+}/(Ce^{3+}+Ce^{4+})$	$O_\beta/(O_\beta+O_\alpha)$
$Ce_{0.35}/TiO_2$	4.63	13.22	82.15	—	22.33	23.42
$Ho_{0.45}Ce_{0.35}/TiO_2$	4.56	12.98	80.35	2.11	31.45	33.25

peak area ratio of the Ce^{3+} and Ce^{4+} peaks. The corresponding results are listed in table 2: $Ho_{0.45}Ce_{0.35}/TiO_2$ (31.45%) and $Ce_{0.35}/TiO_2$ (22.33%). Thus, Ho-doping could promote the transformation of Ce^{4+} to Ce^{3+} over the catalyst surface, which could also effectively improve the SCR activity of $Ce_{0.35}/TiO_2$.

Figure 4*b* shows that the O 1s XPS spectra of $Ce_{0.35}/TiO_2$ and $Ho_{0.45}Ce_{0.35}/TiO_2$ consisted of two peaks, lattice oxygen (binding energy = 529.8 eV, labelled as O_α) and chemisorbed oxygen (binding energy = 532 eV, labelled as O_β) [26,27]. It is well recognized that O_β is more active than O_α in the oxidation reactions of NO to NO_2 [28], which is beneficial for the 'fast SCR' reaction ($NO + NO_2 + 2NH_3 = 2N_2 + 3H_2O$). 'Fast SCR' reaction has been proved conducive to the improvement of the low-temperature SCR activity [29]. The $O_\beta/(O_\alpha + O_\beta)$ ratio was calculated and is presented in table 2. It could be observed that $Ho_{0.45}Ce_{0.35}/TiO_2$ has a bigger $O_\beta/(O_\alpha + O_\beta)$ ratio than $Ce_{0.35}/TiO_2$, which meant that chemisorbed oxygen over the catalyst surface of $Ce_{0.35}/TiO_2$ with Ho modification was obviously improved. Considering the results of the SCR activity and Ce 3d XPS, the O_β ratio result is corresponding with the Ce^{3+} ratio and SCR activity. It may be concluded that more Ce^{3+} was accompanied by an increment of oxygen vacancies and active oxygen species, which played a positive role in the SCR activity. Finally, the XPS spectrum of Ho 4d over $Ho_{0.45}Ce_{0.35}/TiO_2$ is exhibited in figure 4*c*.

3.6. H_2temperature-programmed reduction results

H_2-TPR was performed for studying the redox ability of catalysts. In figure 5, no obvious reduction peak of $Ho_{0.35}/TiO_2$ is observed. The reduction peak of $Ce_{0.35}/TiO_2$ at about 530°C belonged to the reduction of Ce^{4+} to Ce^{3+} [30,31]. With the introduction of Ho to $Ce_{0.35}/TiO_2$, the reduction peak of surface Ce^{4+} moved to lower temperature, which could significantly improve the mobility of surface O owing to the strong synergetic effect between Ti, Ce and Ho species. It was also reported that the synergetic effect could lead to the rise of abundant O defects [32,33]. More O defects were beneficial for the improvement of SCR activity because they could promote O diffusion from the subsurface layer and progressively proceed more in-depth into the bulk [34,35]. It could also be observed that $Ho_{0.45}Ce_{0.35}/TiO_2$ showed the lowest reduction temperature at 446°C and this result is corresponding with its best

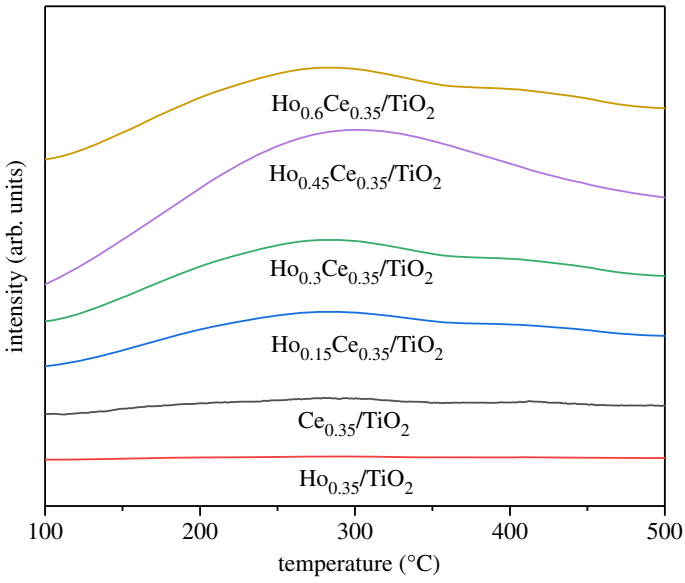

Figure 6. NH_3-TPD patterns of $Ho_xCe_{0.35}/TiO_2$ catalysts.

SCR performance. It seems that further increasing the Ho amount would increase the catalyst reduction temperature. In conclusion, the stronger oxidation–reduction ability of $Ho_{0.45}Ce_{0.35}/TiO_2$ is beneficial for the outstanding SCR reaction performance.

3.7. NH_3 temperature-programmed desorption

Figure 6 shows the effect of Ho modification on NH_3 desorption behaviour of the prepared samples. From figure 6, no obvious desorption peak of $Ho_{0.35}/TiO_2$ was observed and the peak area of $Ce_{0.35}/TiO_2$ is shallow. After the introduction of Ho, the peak surface area gradually increases and the NH_3-TPD profiles existed as a broad peak with the full range of 120–450°C, which included physically adsorbed NH_3, the chemically adsorbed species including adsorbed NH_3 species on Brønsted acid sites and strongly adsorbed on Lewis acid sites [33,36,37]. Thus, more surface sites were available on the $Ce_{0.35}/TiO_2$ surface for NH_3 adsorption after introducing Ho, which could be evidenced by the largest desorption peak area of $Ho_{0.45}Ce_{0.35}/TiO_2$. The phenomenon could also indicate that $Ho_{0.45}Ce_{0.35}/TiO_2$ possesses the most potent surface acidity. Thus the adsorption of NH_3 over it could be boosted and the SCR activity could be promoted correspondingly.

3.8. NO oxidation

Figure 7 exhibits the NO conversion of NO oxidation reaction over the prepared catalysts. It could be easily seen that the NO oxidation conversions over $Ce_{0.35}/TiO_2$ and $Ho_{0.35}/TiO_2$ are very low (below 25%) during 100–400°C, which is consistent with the lowest SCR activity due to the inefficient conversion from NO to NO_2. The activity curves of other catalyst samples demonstrate a parabolic trend, which is an indication of the conversion from the kinetically controlled regime to thermodynamically controlled regime [38]. Especially, $Ho_{0.45}Ce_{0.35}/TiO_2$ has a more significant effect on NO oxidation than other samples. The formation of more NO_2 on the catalyst surface facilitates NOx reduction in the low-temperature range, which was also corresponding with the XPS results. Although $Ho_{0.6}Ce_{0.35}/TiO_2$ had the highest oxidation activity of NO to NO_2 of all samples, it exhibited a relatively lower de-NOx activity compared with $Ho_{0.45}Ce_{0.35}/TiO_2$, which may be attributed to its decreased specific surface area leading to the decreased adsorbed NH_3 species.

3.9. *In situ* diffuse reflectance infrared Fourier transform spectroscopy results

3.9.1. NH_3 adsorption

Figure 8*a* shows the DRIFT spectra of NH_3 adsorption over $Ce_{0.35}/TiO_2$ at different temperatures. The bands at 1599, 1161 cm^{-1} with a shoulder at 1109 cm^{-1} attributed to the coordinated NH_3 linked to

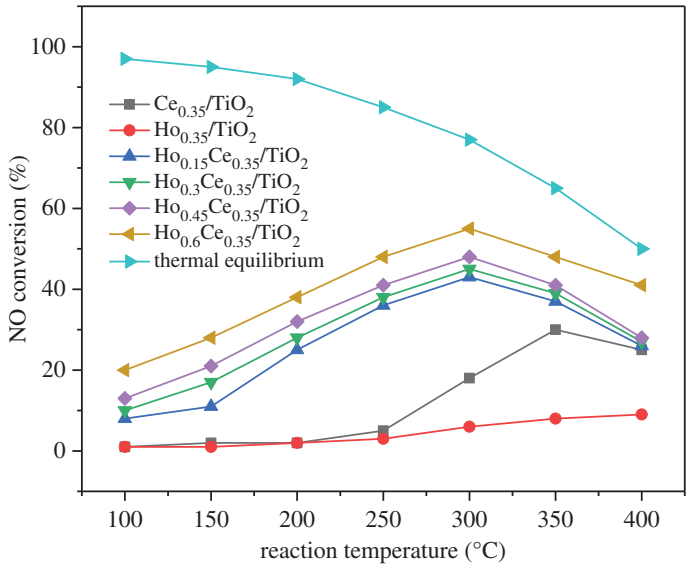

Figure 7. Oxidation activity of NO to NO_2 by O_2 over different catalysts (500 ppm NO, 3 vol.% O_2 and 200 ml min^{-1} total flow rate).

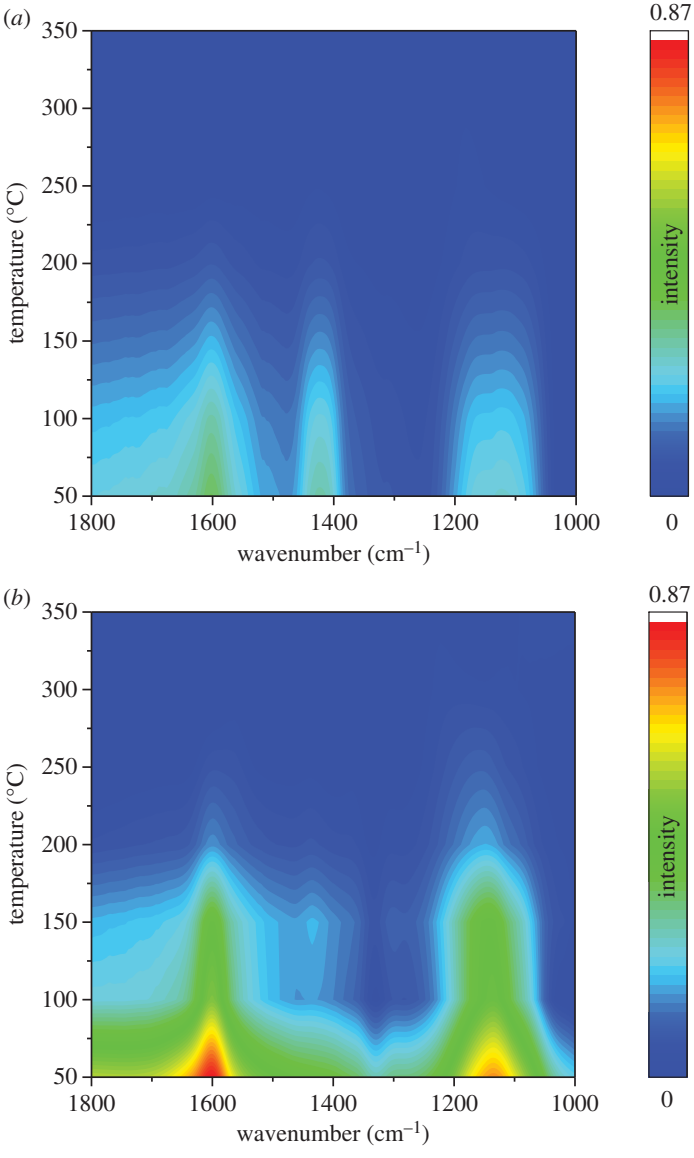

Figure 8. *In situ* DRIFTS of NH_3 adsorption with increasing temperature from 50 to 350°C: (*a*) $Ce_{0.35}/TiO_2$ and (*b*) $Ho_{0.45}Ce_{0.35}/TiO_2$.

Lewis acid sites (NH_3-L) [39,40] could be observed. The band at 1418 cm^{-1} could be assigned to NH_4^+ species on Brønsted acid sites (NH_4^+-B). Notably, all the bands linked to NH_3 species decrease with the temperature increasing owing to the desorption effect.

Figure 8*b* exhibits the DRIFT spectra of NH_3 adsorption over $Ho_xCe_{0.35}/TiO_2$. Similar to the spectra over $Ho_xCe_{0.35}/TiO_2$, the NH_3-L bands (1599 and 1143 cm^{-1}) and the NH_4^+-B band (1432 cm^{-1}) could also be seen. However, the band intensity of adsorbed NH_3 over $Ho_xCe_{0.35}/TiO_2$ was much stronger than that over $Ce_{0.35}/TiO_2$, which indicated that the introduction of Ho species could greatly increase the quantity of both Lewis acid sites and Brønsted acid sites. Previous study by Chen *et al*. [41] and Zhou *et al*. [42] reported that more Brønsted acid sites could help in the generation of adsorbed NH_3 species, thus promoting the low-temperature SCR performance. It should also be noted that the intensity of the bands at 1432 cm^{-1} assigned to Brønsted acid sites in figure 8*b* decreases faster with temperature rising in comparison with those assigned to Lewis acid sites, suggesting NH_3 bonded to Lewis acid sites possessed a better thermostability than that bonded to Brønsted acid sites [41].

3.9.2. $NO + O_2$ adsorption

Figure 9*a* shows the DRIFT spectra of $NO + O_2$ adsorption over $Ce_{0.35}/TiO_2$ at different temperatures. The bands at 1577, 1536 cm^{-1} attributed to bidentate nitrate could be clearly observed; the band at 1599 cm^{-1} could be assigned to ad-NO_2 and the band at 1241 cm^{-1} could be assigned to bridging nitrates [43–45]. It could be observed that all the bands decrease with the temperature increasing owing to the drop in thermal stability.

Figure 9*b* exhibits the DRIFT spectra of $NO + O_2$ adsorption over $Ho_{0.45}Ce_{0.35}/TiO_2$ at different temperatures. As shown in figure 9*b*, the peaks at 1600 cm^{-1} and 1564 cm^{-1} belonged to ad-NO_2 and bidentate nitrate. The peak at 1232 cm^{-1} belonged to bridging nitrates [44]. In comparison with that shown in figure 9*a*, the peak intensity of $Ho_{0.45}Ce_{0.35}/TiO_2$ was stronger than that of $Ce_{0.35}/TiO_2$, which meant that Ho-doping could greatly improve NOx adsorption of $Ce_{0.35}/TiO_2$ catalyst.

3.10. Promotion mechanism

As evidenced by electronic supplementary material, figure S1, all the adsorbed reactants, including ad-NH_3 and ad-NO_X on $Ho_{0.45}Ce_{0.35}/TiO_2$, could participate in the NH_3-SCR reaction. Considering all analysis results given above, doping proper amount of Ho into $Ce_{0.35}/TiO_2$ could generate more active NH_3 and NO_x species on its surface. After adding Ho species, the generation of more Ce^{3+} and O_β over $Ho_{0.45}Ce_{0.35}/TiO_2$ has a facilitation effect on the conversion from NO to NO_2. Thus, the Langmuir–Hinshelwood (L–H) mechanism and Eley–Rideal (E–R) mechanism should be mainly responsible for the promoted low-temperature NH_3-SCR activity over $Ho_{0.45}Ce_{0.35}/TiO_2$, which could be described by the following processes:

(1) L–H mechanism:

$$NO + O_2(g) \rightarrow NO_2(ad) \tag{3.1}$$

$$NH_3(g) \overset{Ce^{4+}}{\rightarrow} NH_3(ad) \quad \text{(Lewis acid sites)}. \tag{3.2}$$

'Fast SCR' reaction:

$$NO_2(ad) + 2NH_3(ad) + NO(g) \rightarrow 2N_2(g) + 3H_2O(g) \tag{3.3}$$

$$NH_3(g) \overset{Ce^{3+}}{\rightarrow} NH_4^+ \text{ (ad) over Brønsted acid sites} \tag{3.4}$$

$$NH_4^+ + e^- + NO_2(ad) \rightarrow NH_4NO_2(ad) \rightarrow N_2 + H_2O. \tag{3.5}$$

(2) E–R mechanism:

$$NH_3(g) \overset{Ce^{4+}}{\rightarrow} NH_3(ad) \quad \text{(on Lewis acid sites)} \tag{3.6}$$

$$O_2(g) \rightarrow 2O(ad) \tag{3.7}$$

$$NH_3(ad) + O(ad) \rightarrow NH_2(ad) + OH(ad) \tag{3.8}$$

$$NO(g) + NH_2(ad) \rightarrow NH_2NO(ad) \tag{3.9}$$

$$NH_2NO(ad) \rightarrow N_2(g) + H_2O. \tag{3.10}$$

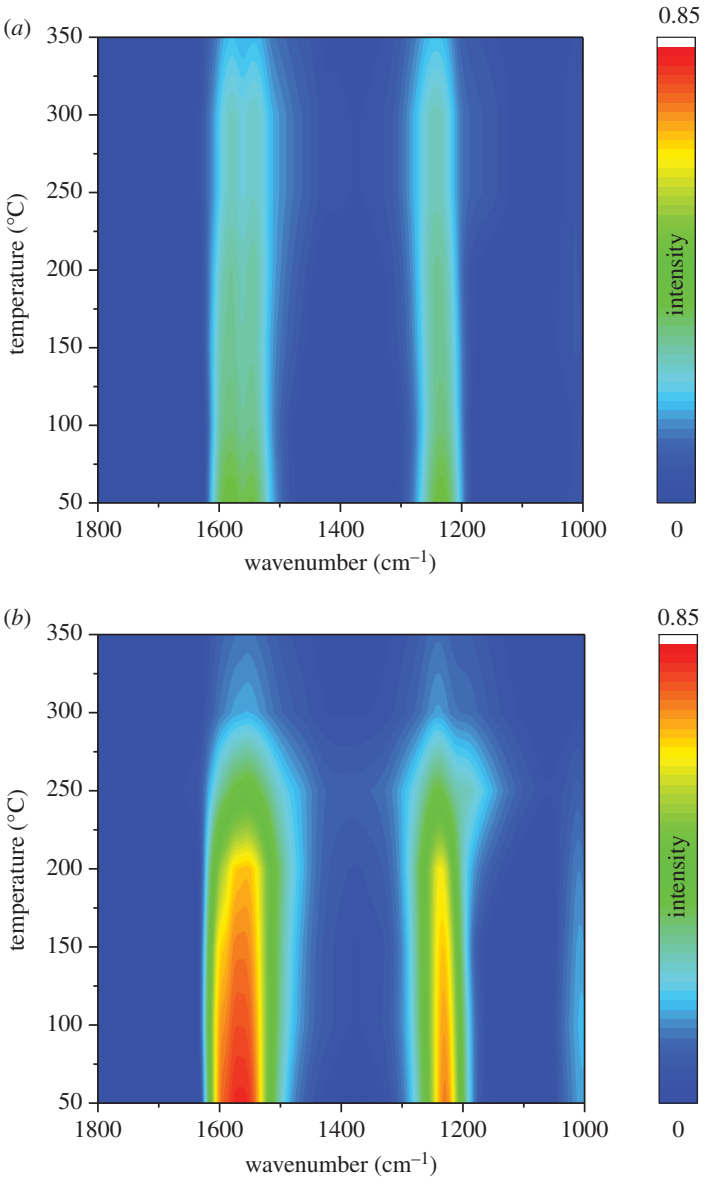

Figure 9. *In situ* DRIFTS of NO + O_2 adsorption with increasing temperature from 50 to 350°C: (*a*) $Ce_{0.35}/TiO_2$ and (*b*) $Ho_{0.45}Ce_{0.35}/TiO_2$.

4. Conclusion

In summary, $Ce_{0.35}/TiO_2$ modified with a certain amount of Ho shows an outstanding low-temperature SCR performance and superior $SO_2 + H_2O$ durability, which could boost the practical application of Ce/TiO_2. *In situ* DRIFTS results revealed that the introduction of Ho species could efficiently promote both active ad-NH_3 and ad-NOx species on $Ce_{0.35}/TiO_2$. Moreover, all of these could contribute to the low-temperature SCR activity of $Ce_{0.35}Ho_{0.45}/TiO_2$ through L–H route and E–R route.

Ethics. Shanghai University Academic Committee approved the study, and the study was also approved by the National Key Research and Development Program of China (no. 2017YFB0404503). Informed consent for the participants to participate in the study has been received. All authors have been personally and actively involved in substantive work leading to the report, and will hold themselves jointly and individually responsible for its content.

Data accessibility. Our data are deposited at: http://dx.doi.org/10.5061/dryad.c86d5m0 [46].

Authors' contributions. T.-t.Z. designed the study, performed the laboratory experiment and wrote the manuscript. L.-m.Y. assisted in analysing experimental data and editing the manuscript for important intellectual content, and gave the final approval for publication.

Competing interests. We declare we have no competing interests.
Funding. Financial support came from the National Key Research and Development Program of China, no. 2017YFB0404503.
Acknowledgements. We are grateful to reviewers who provided comments that substantially improved the manuscript.

References

1. Parks JE. 2010 Less costly catalysts for controlling engine emissions. *Science* **327**, 1584–1585. (doi:10.1126/science.1187154)
2. Koebel M, Elsener M, Kleemann M. 2000 Urea-SCR: a promising technique to reduce NOx emissions from automotive diesel engines. *Catal. Today* **59**, 335–345. (doi:10.1016/S0920-5861(00)00299-6)
3. Pârvulescu VI, Grange P, Delmon B. 1998 Catalytic removal of NO. *Catal. Today* **46**, 233–316. (doi:10.1016/S0920-5861(98)00399-X)
4. Grossale A, Nova I, Tronconi E. 2009 Ammonia blocking of the 'Fast SCR' reactivity over a commercial Fe-zeolite catalyst for diesel exhaust after treatment. *J. Catal.* **265**, 141–147. (doi:10.1016/j.jcat.2009.04.014)
5. Zhao X, Huang L, Li HR, Hu H, Hu XN, Shi LY, Zhang DS. 2016 Promotional effects of zirconium doped $CeVO_4$ for the low-temperature selective catalytic reduction of NOx with NH_3. *Appl. Catal. B* **183**, 269–281. (doi:10.1016/j.apcatb.2015.10.052)
6. Balle P, Geiger B, Kureti S. 2009 Selective catalytic reduction of NOx by NH_3 on Fe/HBEA zeolite catalysts in oxygen-rich exhaust. *Appl. Catal. B* **85**, 109–119. (doi:10.1016/j.apcatb.2008.07.001)
7. Li P, Xin Y, Li Q, Wang Z, Zhang Z, Zheng L. 2012 Ce–Ti amorphous oxides for selective catalytic reduction of NO with NH_3: confirmation of Ce–O–Ti active sites. *Environ. Sci. Technol.* **46**, 9600–9605. (doi:10.1021/es301661r)
8. Li H, Zhang D, Maitarad P, Shi L, Gao R, Zhang J, Cao W. 2012 *In situ* synthesis of 3D flower-like NiMnFe mixed oxides as monolith catalysts for selective catalytic reduction of NO with NH_3. *Chem. Commun.* **48**, 10 645–10 647. (doi:10.1039/C2CC34758J)
9. Djerad S, Crocoll M, Kureti S, Tifouti L, Weisweiler W. 2006 Effect of oxygen concentration on the NOx reduction with ammonia over $V_2O_5–WO_3/TiO_2$catalyst. *Catal. Today* **113**, 208–214. (doi:10.1016/j.cattod.2005.11.067)
10. Paier J, Penschke C, Sauer J. 2013 Oxygen defects and surface chemistry of ceria: quantum chemical studies compared to experiment. *Chem. Rev.* **113**, 3949–3985. (doi:10.1021/cr3004949)
11. Ma Z, Weng D, Wu X, Si Z. 2012 Effects of WOx modification on the activity, adsorption and redox properties of CeO_2 catalyst for NOx reduction with ammonia. *J. Environ. Sci.* **24**, 1305–1316. (doi:10.1016/S1001-0742(11)60925-X)
12. Zhang D, Du X, Shi L, Gao R. 2012 Shape-controlled synthesis and catalytic application of ceria nanomaterials. *Dalton Trans.* **41**, 14 455–14 475. (doi:10.1039/C2DT31759A)
13. Gao X, Jiang Y, Fu Y, Zhong Y, Luo Z, Cen K. 2010 Preparation and characterization of CeO_2/TiO_2 catalysts for selective catalytic reduction of NO with NH_3. *Catal. Commun.* **11**, 465–469. (doi:10.1016/j.catcom.2009.11.024)
14. Vuong TH, Radnik JR, Rabeah J, Bentrup U, Schneider M, Atia H, Armbruster U, Grünert W, Brückner A. 2017 Efficient $VOx/Ce_{1-x}TixO_2$ catalysts for low-temperature NH_3-SCR: reaction mechanism and active sites assessed by *in situ*/operando spectroscopy. *ACS Catal.* **7**, 1693–1705. (doi:10.1021/acscatal.6b03223)
15. Jiang Y, Wang X, Lai C, Shi W, Liang G, Bao C, Ma S. 2018 Effect of Ca doping on the selective catalytic reduction of NO with NH_3 over Ce–Ti oxide catalyst. *Catal. Lett.* **148**, 2911–2917. (doi:10.1007/s10562-018-2494-1)
16. Mosrati J *et al.* 2018 Nb-modified Ce/Ti oxide catalyst for the selective catalytic reduction of NO with NH_3 at low temperature. *Catalysts* **8**, 175. (doi:10.3390/catal8050175)
17. Du XS, Gao X, Cui LW, Fu YC, Luo ZY, Cen, KF 2012 Investigation of the effect of Cu addition on the SO_2-resistance of a CeTi oxide catalyst for selective catalytic reduction of NO with NH_3. *Fuel* **92**, 49–55. (doi:10.1016/j.fuel.2011.08.014)
18. Xie Y, Yuan C. 2003 Visible-light responsive cerium ion modified titania sol and nanocrystallites for X-3B dye photodegradation. *Appl. Catal. B* **46**, 251–259. (doi:10.1016/S0926-3373(03)00211-X)
19. Mekhemer GA. 2004 Surface acid–base properties of holmium oxide catalyst: *in situ* infrared spectroscopy. *Appl. Catal. A* **275**, 1–7. (doi:10.1016/j.apcata.2004.05.036)
20. Zhu Y, Zhang Y, Xiao R, Huang T, Shen K. 2017 Novel holmium-modified $Fe-Mn/TiO_2$ catalysts with a broad temperature window and high sulfur dioxide tolerance for low-temperature SCR. *Catal. Commun.* **88**, 64–67. (doi:10.1016/j.catcom.2016.09.031)
21. Liu Z, Zhang S, Li J, Ma L. 2014 Promoting effect of MoO_3 on the NOx reduction by NH_3 over CeO_2/TiO_2 catalyst studied with *in situ* DRIFTS. *Appl. Catal. B* **144**, 90–95. (doi:10.1016/j.apcatb.2013.06.036)
22. Burroughs P, Hamnett A, Orchard AF, Thornton G. 1976 Satellite structure in the X-ray photoelectron spectra of some binary and mixed oxides of lanthanum and cerium. *J. Chem. Soc. Dalton Trans.* 1686–1698. (doi:10.1039/DT9760001686)
23. Chen X, Geng Y, Shan W, Liu F. 2018 Deactivation effects of potassium on a CeMoTiOx catalyst for the selective catalytic reduction of NOx with NH_3. *Ind. Eng. Chem. Res.* **57**, 1399–1407. (doi:10.1021/acs.iecr.7b04444)
24. Liu Z, Yi Y, Li J, Woo SI, Wang B, Cao X, Li Z. 2013 A superior catalyst with dual redox cycles for the selective reduction of NOx by ammonia. *Chem. Commun.* **49**, 7726–7728. (doi:10.1039/C3CC43041C)
25. Liu C, Chen L, Chang H, Ma L, Peng Y, Arandiyan H, Li J. 2013 Characterization of $CeO_2–WO_3$ catalysts prepared by different methods for selective catalytic reduction of NOx with NH_3. *Catal. Commun.* **40**, 145–148. (doi:10.1016/j.catcom.2013.06.017)
26. Dupin JC, Gonbeau D, Vinatier P, Levasseur A. 2000 Systematic XPS studies of metal oxides, hydroxides and peroxides. *Phys. Chem. Chem. Phys.* **2**, 1319–1324. (doi:10.1039/A908800H)
27. Eom Y, Jeon SH, Ngo TA, Kim J, Lee TG. 2008 Heterogeneous mercury reaction on a selective catalytic reduction (SCR) catalyst. *Catal. Lett.* **121**, 219–225. (doi:10.1007/s10562-007-9317-0)
28. Wu Z, Jin R, Liu Y, Wang H. 2008 Ceria modified $MnOx/TiO_2$ as a superior catalyst for NO reduction with NH_3 at low-temperature. *Catal. Commun.* **9**, 2217–2220. (doi:10.1016/j.catcom.2008.05.001)
29. Kato A, Matsuda S, Kamo T, Nakajima F, Kuroda H, Narita T. 1981 Reaction between nitrogen oxide (NOx) and ammonia on iron oxide-titanium oxide catalyst. *J. Phys. Chem.* **85**, 4099–4102. (doi:10.1021/j150626a029)
30. Li X, Li Y. 2014 Selective catalytic reduction of NO with NH_3 over Ce–Mo–Ox catalyst. *Catal. Lett.* **144**, 165–171. (doi:10.1007/s10562-013-1103-6)
31. Peng Y, Li J, Chen L, Chen J, Han J, Zhang H, Han W. 2012 Alkali metal poisoning of a $CeO_2–WO_3$ catalyst used in the selective catalytic reduction of NOx with NH_3: an experimental and theoretical study. *Environ. Sci. Technol.* **46**, 2864–2869. (doi:10.1021/es203619w)
32. Cai S, Zhang D, Zhang L, Huang L, Li H, Gao R, Shi L, Zhang J. 2014 Comparative study of 3D ordered macroporous $Ce_{0.75}Zr_{0.2}M_{0.05}O_{2-\delta}$ (M= Fe, Cu, Mn, Co) for selective catalytic reduction of NO with NH_3. *Catal. Sci. Technol.* **4**, 93–101. (doi:10.1039/C3CY00398A)
33. Xu H, Wang Y, Cao Y, Fang Z, Lin T, Gong M, Chen Y. 2014 Catalytic performance of acidic zirconium-based composite oxides monolithic catalyst on selective catalytic reduction of NOx with NH_3. *Chem. Eng. J.* **240**, 62–73. (doi:10.1016/j.cej.2013.11.053)
34. Yu J, Si Z, Chen L, Wu X, Weng D. 2015 Selective catalytic reduction of NOx by ammonia over phosphate-containing $Ce_{0.75}Zr_{0.25}O_2$ solids. *Appl. Catal. B* **163**, 223–232. (doi:10.1016/j.apcatb.2014.08.006)

35. Christou S, Álvarez-Galván M, Fierro J, Efstathiou A. 2011 Suppression of the oxygen storage and release kinetics in $Ce_{0.5}Zr_{0.5}O_2$ induced by P, Ca and Zn chemical poisoning. *Appl. Catal. B* **106**, 103–113. (doi:10.1016/j.apcatb.2011.05.013)
36. Pena DA, Uphade BS, Smirniotis PG. 2004 TiO_2-supported metal oxide catalysts for low-temperature selective catalytic reduction of NO with NH_3: I. Evaluation and characterization of first row transition metals. *J. Catal.* **221**, 421–431. (doi:10.1016/j.jcat.2003.09.003)
37. Roy S, Viswanath B, Hegde M, Madras G. 2008 Low-temperature selective catalytic reduction of NO with NH_3 over $Ti_{0.9}M_{0.1}O_{2-\delta}$ (M= Cr, Mn, Fe, Co, Cu). *J. Phys. Chem. C* **112**, 6002–6012. (doi:10.1021/jp7117086)
38. Tang N, Liu Y, Wang H, Wu Z. 2011 Mechanism study of NO catalytic oxidation over MnO_x/TiO_2 catalysts. *J. Phys. Chem. C* **115**, 8214–8220. (doi:10.1021/jp200920z)
39. Lietti L, Nova I, Ramis G, Dall'Acqua L, Giamello E, Forzatti P, Bregani F. 1999 Characterization and reactivity of V_2O_5-MoO_3/TiO_2 de-NOx SCR catalysts. *J. Catal.* **187**, 419–435. (doi:10.1006/jcat.1999.2603)
40. Larrubia MA, Ramis G. 2000 An FT-IR study of the adsorption of urea and ammonia over $V_2O_5-MoO_3-TiO_2$ SCR catalysts. *Appl. Catal. B* **27**, 145–151. (doi:10.1016/S0926-3373(00)00150-8)
41. Chen L, Li J, Ge M. 2010 DRIFT study on cerium—tungsten/titiania catalyst for selective catalytic reduction of NOx with NH_3. *Environ. Sci. Technol.* **44**, 9590–9596. (doi:10.1021/es102692b)
42. Zhou G, Zhong B, Wang W, Guan X, Huang B, Ye D, Wu H. 2011 *In situ* DRIFTS study of NO reduction by NH_3 over Fe–Ce–Mn/ZSM-5 catalysts. *Catal. Today* **175**, 157–163. (doi:10.1016/j.cattod.2011.06.004)
43. Wu Z, Jiang B, Liu Y, Wang H, Jin R. 2007 DRIFT study of manganese/titania-based catalysts for low-temperature selective catalytic reduction of NO with NH_3. *Environ. Sci. Technol.* **41**, 5812–5817. (doi:10.1021/es0700350)
44. Adamowska M, Krztoń A, Najbar M, Da Costa, P, Djéga-Mariadassou G. 2008 DRIFT study of the interaction of NO and O_2 with the surface of $Ce_{0.62}Zr_{0.38}O_2$ as deNOx catalyst. *Catal. Today* **137**, 288–291. (doi:10.1016/j.cattod.2008.01.013)
45. Kijlstra WS, Brands DS, Smit HI, Poels EK, Bliek A. 1997 Mechanism of the selective catalytic reduction of NO with NH_3 over $MnOx/Al_2O_3$. *J. Catal.* **171**, 219–230. (doi:10.1016/S0920-5861(98)00470-2)
46. Zhang T, Yan L. 2019 Data from: Enhanced low-temperature NH3-SCR performance of Ce/TiO2 modified by Ho catalyst. Dryad Digital Repository. (doi:10.5061/dryad.c86d5m0)